

gion exceeds 12 GV from all directions of incidence, we conclude tentatively that these electrons are either the product of pion decay from cosmic-ray interactions with ring material, or the atmosphere of Saturn, or—more likely—trapped electrons that were first accelerated beyond the radius of the A ring and, subsequently, have been scattered in the magnetic field at high latitudes into $L \leq 2.3$.

Conclusions. We have discovered that, as at Earth and Jupiter, the magnetosphere of Saturn contains high-energy trapped nucleons and electrons and, as at Jupiter, radiation is absorbed by planetary satellites. Peak intensities of electrons and protons in these magnetospheres are shown in Table 2, and it is clear that the maximum trapped radiation intensities observed for Saturn lie between those of Earth and Jupiter. For the Pioneer 11 trajectory the fluence of > 3.4 MeV electrons was $9.1 \times 10^9 \text{ cm}^{-2}$ [corresponding to 290 radiation units (silicon)].

Our data contain evidence for a new satellite of Saturn with a semimajor axis of $2.51 R_S$ —the first satellite to be discovered from analysis of energetic charged particle radiation. There also are absorption features, for example, at the orbit of Mimas and at the F ring, which may be accounted for by unknown satellites or clumps of ring material. The width and inbound-outbound symmetry of the observed absorption features are consistent with a spin-aligned dipole magnetic moment offset from the rotation axis by no more than $0.01 R_S$. In some cases the radiation intensity profile appears to be inconsistent with predictions of a steady-state inward diffusion model for populating the inner-trapped radiation zones.

We conclude that the inner Saturn magnetosphere, because of its near-axial symmetry and the many discrete radiation absorption regions, offers a unique opportunity to study the acceleration and transport of charged particles in a planetary magnetic field. These and other questions, such as the strong and changing particle anisotropies that we have observed but have not discussed herein, will be discussed elsewhere.

J. A. SIMPSON
T. S. BASTIAN
D. L. CHENETTE
G. A. LENTZ
R. B. MCKIBBEN
K. R. PYLE
A. J. TUZZOLINO

Enrico Fermi Institute,
University of Chicago,
Chicago, Illinois 60637

References and Notes

1. J. W. Dyer, *Science* **207**, 400 (1980).
2. J. A. Simpson and R. B. McKibben, in *Jupiter*, T. Gehrels, Ed. (Univ. of Arizona Press, Tucson, 1976), pp. 738–766.
3. J. A. Simpson *et al.*, *J. Geophys. Res.* **79**, 3522 (1974).
4. J. A. Simpson, J. H. Eraker, J. E. Lamport, P. H. Walpole, *Science* **185**, 160 (1974).
5. L. W. Brown, *Astrophys. J.* **198**, L89 (1975).
6. C. F. Kennel, *Space Sci. Rev.* **14**, 511 (1973).
7. G. Siscoe, in *Solar System Plasma Physics*, C. Kennel, L. J. Lanzerotti, E. N. Parker, Eds. (North-Holland, Amsterdam, 1979), p. 319.
8. J. A. Simpson, G. A. Lentz, R. B. McKibben, J. J. O'Gallagher, W. Schroeder, A. J. Tuzzolino, *NSSDC Tech. Ref. File B21970* (Goddard Space Flight Center, Greenbelt, Md., 1974).
9. E. J. Smith, L. Davis, Jr., D. E. Jones, P. J. Coleman, Jr., D. S. Colburn, P. Dyal, C. P. Sonnett, *Science* **207**, 407 (1980).
10. Electrons > 3.4 MeV are measured by the ECD (3) with a calibration revised since the Pioneer 10 and 11 Jupiter encounters (3).
11. J. H. Wolfe, J. D. Mihalov, H. R. Collard, D. D. McKibbin, L. A. Frank, D. S. Intriligator, *Science* **207**, 411 (1980).
12. J. A. Simpson, D. Hamilton, G. Lentz, R. B. McKibben, A. Mogro-Campero, M. Perkins, K. R. Pyle, A. J. Tuzzolino, J. J. O'Gallagher, *ibid.* **183**, 306 (1974).
13. J. A. Simpson, D. C. Hamilton, G. A. Lentz, R. B. McKibben, M. Perkins, K. R. Pyle, A. J. Tuzzolino, J. J. O'Gallagher, *ibid.* **188**, 455 (1975).
14. W. A. Feibelman, *Nature (London)* **214**, 793 (1967).
15. M. F. Thomsen and J. A. Van Allen, *Geophys. Res. Lett.* **6**, 893 (1979).

16. F. A. Franklin, G. Colombo, A. F. Cook, *Icarus* **15**, 80 (1971).
17. A. Dollfus, *Astronomie* **6**, 253 (1968).
18. J. W. Fountain and S. M. Larson, *Science* **197**, 915 (1977).
19. J. A. Van Allen, M. F. Thomsen, B. A. Randall, R. L. Rairden, C. L. Grosskreutz, *Science* **207**, 415 (1980).
20. W. Fillius, W. H. Ip, C. E. McIlwain, *ibid.*, p. 425.
21. J. A. Simpson, news conference, 4 September 1979; *Trans. Am. Geophys. U.* **60**, 865 (1979).
22. J. A. Anderson, G. W. Null, E. D. Biller, S. K. Wong, W. B. Hubbard, J. J. MacFarlane, *Science* **207**, 449 (1980).
23. T. Gehrels *et al.*, *Science* **207**, 434 (1980).
24. James B. Pollack, *Space Sci. Rev.* **18**, 3 (1975).
25. W. N. Hess, *The Radiation Belt and Magnetosphere* (Blaisdell, Waltham, Mass., 1968).
26. D. Morrison, D. P. Cruikshank, J. A. Burns, in *Planetary Satellites*, J. A. Burns, Ed. (Univ. of Arizona Press, Tucson, 1977), pp. 3–17.
27. We are grateful to the Pioneer Project Office, especially to C. F. Hall, R. Hogan, and J. Dyer, and to the staff of the Laboratory for Astrophysics and Space Research of the Enrico Fermi Institute, particularly M. Perkins, R. Jacquet, and J. Lamport for their contributions to the instrumentation. We appreciate the assistance and advice of J. J. O'Gallagher, S. P. Christon, J. H. Eraker, S. Tejero, J. Cooper, and P. Kruley during the Saturn encounter and during the preparation of this report. We thank J. H. Wolfe and E. J. Smith for making available to us their preliminary plasma and magnetic field data, respectively. This work was supported in part by NASA/Ames NAS 2-6551 contract, NASA grant NGL 14-001-006, and NSF grant ATM 77-24494.

3 December 1979

Saturn's Magnetosphere, Rings, and Inner Satellites

Abstract. Our 31 August to 5 September 1979 observations together with those of the other Pioneer 11 investigators provide the first credible discovery of the magnetosphere of Saturn and many detailed characteristics thereof. In physical dimensions and energetic charged particle population, Saturn's magnetosphere is intermediate between those of Earth and Jupiter. In terms of planetary radii, the scale of Saturn's magnetosphere more nearly resembles that of Earth and there is much less inflation by entrapped plasma than in the case at Jupiter. The orbit of Titan lies in the outer fringes of the magnetosphere. Particle angular distributions on the inbound leg of the trajectory (sunward side) have a complex pattern but are everywhere consistent with a dipolar magnetic field approximately perpendicular to the planet's equator. On the outbound leg (dawnside) there are marked departures from this situation outside of 7 Saturn radii (R_S), suggesting an equatorial current sheet having both longitudinal and radial components. The particulate rings and inner satellites have a profound effect on the distribution of energetic particles. We find (i) clear absorption signatures of Dione and Mimas; (ii) a broad absorption region encompassing the orbital radii of Tethys and Enceladus but probably attributable, at least in part, to plasma physical effects; (iii) no evidence for Janus (1966 S 1) (S 10) at or near $2.66 R_S$; (iv) a satellite of diameter ≥ 170 kilometers at $2.534 R_S$ (1979 S 2), probably the same object as that detected optically by Pioneer 11 (1979 S 1) and previously by ground-based telescopes (1966 S 2) (S 11); (v) a satellite of comparable diameter at $2.343 R_S$ (1979 S 5); (vi) confirmation of the F ring between 2.336 and $2.371 R_S$; (vii) confirmation of the Pioneer division between 2.292 and $2.336 R_S$; (viii) a suspected satellite at $2.82 R_S$ (1979 S 3); (ix) no clear evidence for the E ring though its influence may be obscured by stronger effects; and (x) the outer radius of the A ring at $2.292 R_S$. Inside of $2.292 R_S$ there is a virtually total absence of magnetospheric particles and a marked reduction in cosmic-ray intensity. All distances are in units of the adopted equatorial radius of Saturn, 60,000 kilometers.

We report herein the discovery of the magnetosphere of Saturn and a survey of its characteristics. In addition, new findings on the rings and inner satellites of the planet are provided by the measurements of energetic charged particle distributions within the inner magneto-

sphere. Before Pioneer 11's flyby encounter with Saturn (periapsis on 1 September 1979) (1) there was only meager observational evidence on the basic question of whether or not this planet is magnetized (2, 3).

The University of Iowa instrument on

Pioneer 11 was described previously (4, 5), and the basic characteristics of the detectors and other relevant information are summarized in (6) and in Table 1. Figure 1 shows 15-minute averaged, dead-time-corrected counting rates of detectors A, B, C, D, and G.

A solar energetic particle event had been in progress for about 10 days before

the first detection of effects attributable to Saturn. Coincidentally a marked increase in solar wind pressure occurred on day of year 240. Three successive bow-shock crossings were identified on day of year 243 with the plasma analyzer (7) and the magnetometer (8). These (BS in Fig. 1) occurred at radial distances of 24.1, 23.1, and 20.0 R_S , respectively.

There were barely discernible peaks in the intensity of electrons $E_e > 40$ keV at these times.

The major features of our subsequent data are as follows.

1) The trapping boundary for energetic particles, as shown most clearly by our low-energy electron detector ($E_e > 40$ keV), is accurately coincident with the magnetopause as defined by data from the plasma analyzer and the magnetometer. The intensity of such electrons increases dramatically just inside the magnetopause on both inbound and outbound legs of the encounter trajectory.

2) The radial distances to the magnetopause (MP in Fig. 1) on both inbound (17.3 R_S) (local time 11.6 hours) and outbound (30.3 to 39.8 R_S) (local time 6.3 hours) legs of the encounter trajectory are compatible with simple theoretical expectations for a vacuum dipole of moment 0.21 gauss R_S^3 (8, 9) and the prevailing solar wind pressure (7). Hence, inflation of the magnetosphere by trapped plasma is considerably less important than in Jupiter's magnetosphere (4, 5).

3) The rings and inner satellites of Saturn have a profound effect on limiting the increase in charged particle intensities as the radial distance diminishes. The absorption "signatures" in curves for particle intensity plotted against time (or radial distance) provide (i) very valuable diagnostics on magnetospheric processes (for example, diffusion coefficients and loss rates) and (ii) a new technique (particle beam astronomy) for discovering previously unknown satellites and rings and for confirming or contradicting reports of such objects based on optical evidence.

4) The observed dimensions of Saturn's magnetosphere (perhaps ≈ 50 percent smaller than average because of markedly enhanced solar wind pressure at the time of the Pioneer 11 encounter) are such that Titan's orbit lies in its outer fringe.

5) No overall periodic modulation of particle intensities at the assumed 10 hour 14 minute rotational period of the planet has been found. This result is compatible with the finding of both magnetometer groups (8, 9) that the dipole axis is tilted less than 1° to the planet's rotational axis.

6) Appreciable intensities of electrons $E_e > 21$ MeV or protons $E_p > 80$ MeV, or both, exist only between about 5.8 and 2.292 R_S with a maximum at 2.66 R_S both inbound and outbound.

7) There is a virtually total absence of magnetospheric particles within a radial distance of 2.292 R_S , corresponding to

Table 1. Energy ranges and geometric factors for Pioneer 11 detectors.

Detector	Effective energy range (MeV)	Effective inverse omnidirectional geometric factor* ($1/Q$), cm^{-2}	Type	$1/4\pi Q$ ($\text{cm}^2 \text{sr}^{-1}$) ⁻¹
<i>Electrons</i>				
A - C	$0.040 < E_e < 21$	730	Directional	58.1
B - C	$0.56 < E_e < 21$	785	Directional	62.5
G	InSENSITIVE			
C	$E_e > 21$	23	Omnidirectional	
D	$E_e > 31$	63	Omnidirectional	
<i>Protons</i>				
A - C	$0.61 < E_p < 80$	650	Directional	51.7
B - C	$9 < E_p < 80$	650	Directional	51.7
G	$0.61 < E_p < 3.41$	285	Directional	22.7
C	$E_p > 80$	8.2	Omnidirectional	
D	$E_p > 80$	23	Omnidirectional	

*The absolute omnidirectional intensity I in $(\text{cm}^2 \text{sec})^{-1}$ is approximated by the product of the spin-averaged counting rate by $(1/Q)$. The absolute spin-averaged unidirectional intensity j in $(\text{cm}^2 \text{sec sr})^{-1}$ is approximated by the product of the spin-averaged counting rate by $(1/4\pi Q)$.

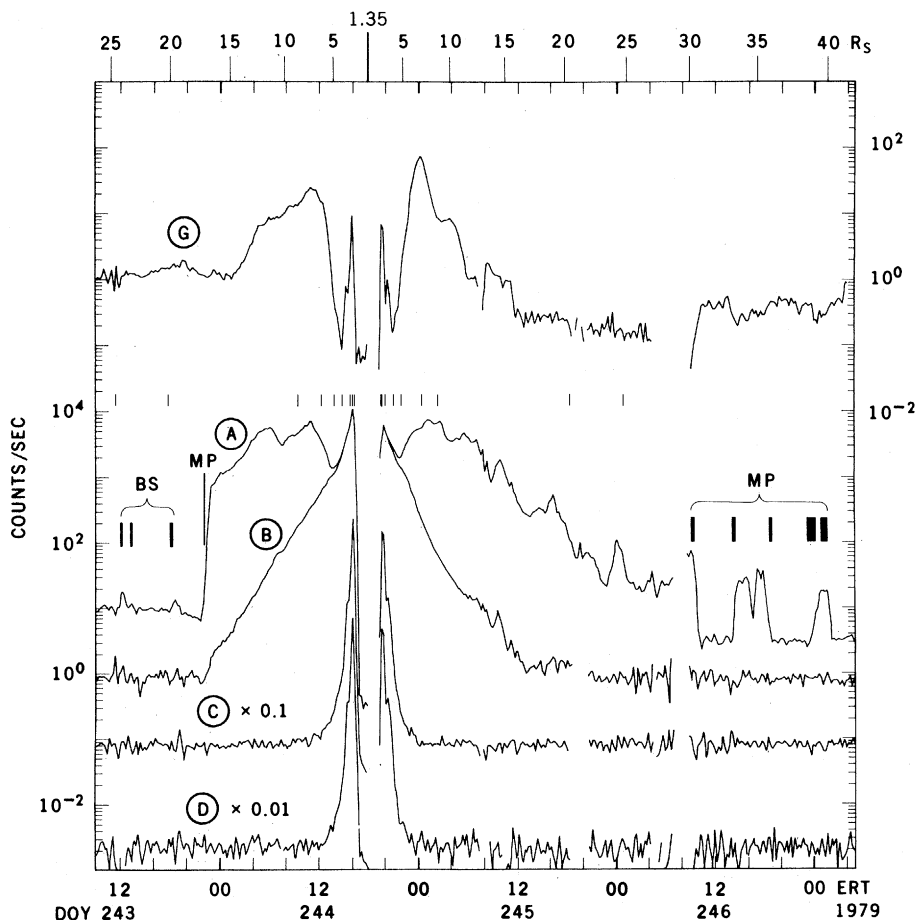


Fig. 1. General overview of 15-minute corrected counting rates of University of Iowa detectors A, B, C, D, and G [see Table 1 and (6)]. The vertical ticks in the upper center of the diagram show the semimajor axes of previously identified satellites, starting with Titan on each end and reading inward.

the outer edge of the A ring. At this boundary intensities decrease by a factor of ~ 1000 within a radial distance of $0.01 R_S$. Also, the intensity of galactic cosmic rays is markedly reduced within the inner void, presumably by the planet's general magnetic field. (Equatorial values of the vertical Stoermer momentum cutoff for protons are $pc = 24$ BeV at $2.0 R_S$ and 95 BeV at $1.0 R_S$, using a magnetic moment of 0.21 gauss R_S^3 .)

8) The fluence of electrons $E_e > 0.56$ MeV integrated through the entire Pioneer 11 encounter was $6.6 \times 10^{10} \text{ cm}^{-2}$. This corresponds to about 2300 roentgens.

Absorption features. A portion of the curve for the (115.5-second averaged) counting rate plotted against time for detector G is shown on an expanded scale in Fig. 2 (inbound). The vertical arrows labeled Dione, Tethys, Enceladus, and Mimas are placed at radial distances equal to the semimajor axes of their well-established orbits. The energetic particle signatures (that is, dips in intensity) of Dione and Mimas correspond quite accurately to their orbits. The signatures of the particle absorption effects of Tethys and Enceladus are not resolved. The broad depression of proton intensity appears to be attributable to a composite effect of these two satellites, though there may be important plasma physical effects in addition. The corresponding outbound curve is almost identical over the region shown.

Figure 3 (115.5-second averaged data) shows both inbound and outbound counting rates for our two high-energy particle detectors. A clear and well-defined signature of Mimas is shown. By virtue of both Figs. 2 and 3 and using Mimas's signature as a calibration and validation of our technique, we identify the feature at $2.82 R_S$ as provisional evidence for a heretofore unknown satellite (1979 S 3).

A further expansion of scale is given in Fig. 4 [individual frame-by-frame counting rates at our ultimate time resolution, as described in (6)]. In no one of Figs. 2, 3, and 4 is there any evidence for the existence of Janus (S 10 or 1966 S 1) at or near $2.66 R_S$.

There is a major absorption feature centered at about $2.52 R_S$. The depressed value of the intensity of energetic particles is approximately constant over the radial range 2.550 to $2.490 R_S$. Within this range at $2.534 R_S$ inbound, we observed a dramatic and very brief reduction in counting rates of detectors A, B, C, and D. (The counting rate of G, as shown in Fig. 2, was already too low to show this detailed feature.) By virtue of

the sequential sampling of the various detectors, it has been possible to construct a detailed profile of this fine-scale absorption feature, as shown in the lower portion of Fig. 4. The time width of the profile at $1/e$ of its normalized ambient intensity is 10 seconds. At this time, the radial component of the velocity of the spacecraft was 16.82 km/sec, and the spacecraft was 2300 km south of the ring plane. Thus the apparent radial dimension of this feature is 170 km if it is bounded by two magnetic shells or ≥ 170 km if it is bounded by a magnetic tube of force. The presence of this marked absorption (99 percent of the am-

bient intensity) was discovered by R. L. Rairden while he was plotting the frame-by-frame Iowa data in nearly real time.

Despite the brevity of these effects we have found no basis for not accepting them as valid. Two of the other Pioneer 11 particle investigators subsequently found similar effects (10, 11). We interpret the deep absorption feature at 1618:14 Earth received time (ERT) ($2.534 R_S$) as the particle shadow [see Van Allen and Ness (12) for particle shadows by Earth's moon] of a satellite of diameter ≥ 170 km (1979 S 2). Because of the combined effects of corotational motion and magnetic curvature

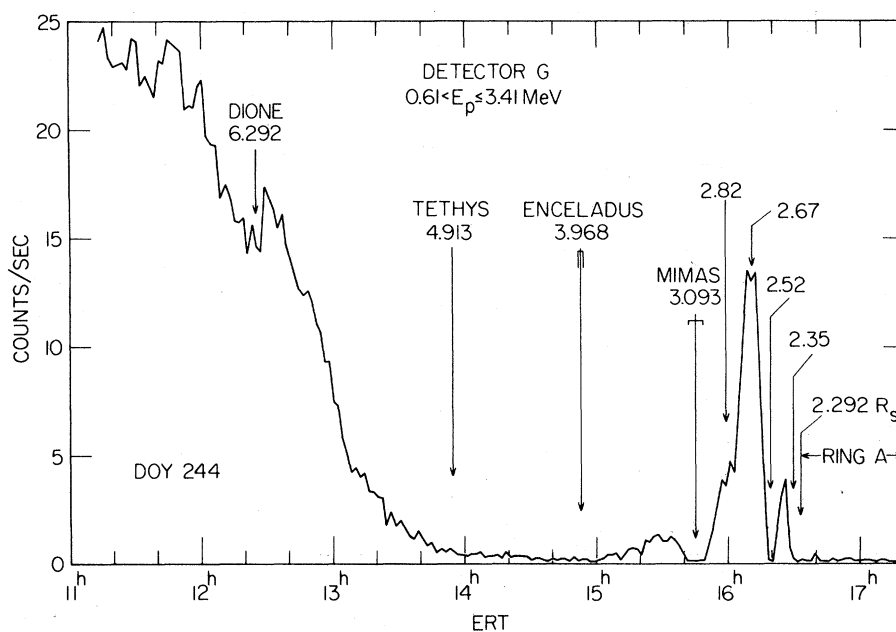


Fig. 2. Plot of 115.5-second averaged counting rates of G, inbound. Vertical arrows show semimajor axes of Dione, Tethys, Enceladus, and Mimas (the last two with horizontal bars showing eccentricity of their orbits) and other features of interest as described in the text.

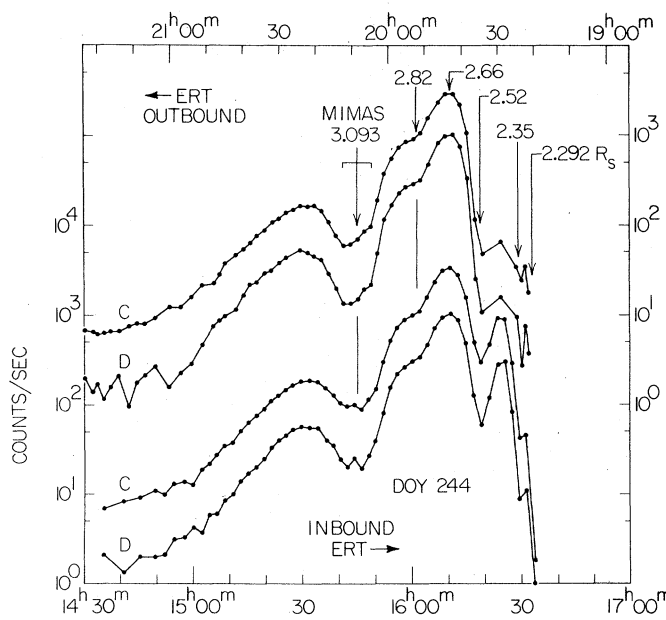


Fig. 3. Plots of 115.5-second averaged counting rates of energetic particle detectors C and D, both inbound and outbound. The time scales are matched so that the abscissa corresponds to the same radial distance on all four curves.

and gradient drift, electrically charged particles in general have a net longitudinal velocity relative to an orbiting satellite. Thus the "hole" (a vacant magnetic tube of force) that is created in the distri-

bution of particles when they are absorbed by the satellite will stretch out longitudinally relative to the satellite as the particles drift past. For electrons at $2.534 R_S$ with energies above about 1

MeV, this shadow region extends westward (retrograde sense) from the satellite. The longitudinal length of the extended shadow is dependent on the rate at which it is refilled by radial diffusion. Our preliminary consideration of these effects suggests that the spacecraft crossed the orbital radius of the satellite within a few degrees of longitude westward of the satellite. If this is confirmed by more thorough analysis, it appears likely that 1979 S 2 is the same body as 1979 S 1 observed 16 hours previously by the imaging photopolarimeter team (13).

A further absorption signature on our detector D (only) occurs at $2.522 R_S$ outbound (Fig. 4) (probability of less than 1 percent of being a statistical fluctuation). This may be caused by another satellite (1979 S 4) in an orbit similar to that of 1979 S 2 or it may be the longitudinally extended shadow of 1979 S 2. The orbital radii of 1979 S 1, S 2, and S 4 are all consistent with the Fountain-Larson object 1966 S 2 (also called S 11) (14). The entire broad absorption feature between 2.490 and $2.550 R_S$ may conceivably be caused by a single satellite, with its radial width ($0.06 R_S$) being attributable to orbital eccentricity of the satellite and to offset of the magnetic center of the planet from its geometric center. An alternative view is that there may be several or many small satellites (tens of kilometers or more in diameter) within this region as suggested by Aksnes and Franklin (15).

Figure 5 shows another segment of the data at our highest time resolution. The sinusoidal variation of the rates of directional detectors A and B is the result of sweeping their axes through an anisotropic (pancake) distribution of intensities; the 58-second periodicity is the "beat note" between the spin period 7.693 seconds and the sampling period 8.250 seconds. The most striking feature here is the dramatic cutoff of intensity at the outer edge of the A ring—by a factor of ≈ 1000 within $0.01 R_S$. The dashed curve, calculated for loss-free diffusion with a perfect absorber at radius r_c , fits the upper envelope of either the A or B rates and provides a means of refining the value of r_c . A value of $r_c = 2.292$ (± 0.002) R_S or $137,520 \pm 120$ km is found for the radius of the outer edge of the A ring. Inasmuch as our particle absorption technique is probably more sensitive to diffuse matter than either the imaging photopolarimeter (13) or infrared instrument (16), the difference between the value, $2.27 R_S$, obtained with those instruments, and our value of $2.292 R_S$ for the apparent outer radius of the A ring places an upper limit on the equatorial plane offset of the magnetic center from

Table 2. New information on satellites and rings ($1 R_S = 60,000$ km).

Feature	Radial distance*	Remarks
Outer-edge of the A ring	2.292	
Pioneer division	2.292 to 2.336	
Absorption feature	2.336 to 2.371	Confirmatory of the F ring
Satellite 1979 S 5	2.343	Firmly established
Satellite 1979 S 6	2.350	May be longitudinally extended signature of S 5
Satellite 1979 S 2	2.534	Firmly established
Satellite 1979 S 4	2.522	May be longitudinally extended signature of S 2
Both S 2 and S 4 absorption signatures may be attributable to optically detected object 1979 S 1 which in turn may be 1966 S 2 (S 11)		
Satellite 1979 S 3	2.82	Suspected but interpretation of signature ambiguous
Satellite 1966 S 1 (S 10) is not confirmed at or near 2.66		
E ring is not confirmed but may be obscured by other stronger effects		

*All radial distances at point of observation are in units of planet's adopted equatorial radius with an observational uncertainty of ± 0.002 . Interpretative uncertainties involve unknown offset of magnetic center from geometrical center of the planet and unknown eccentricities of satellite orbits.

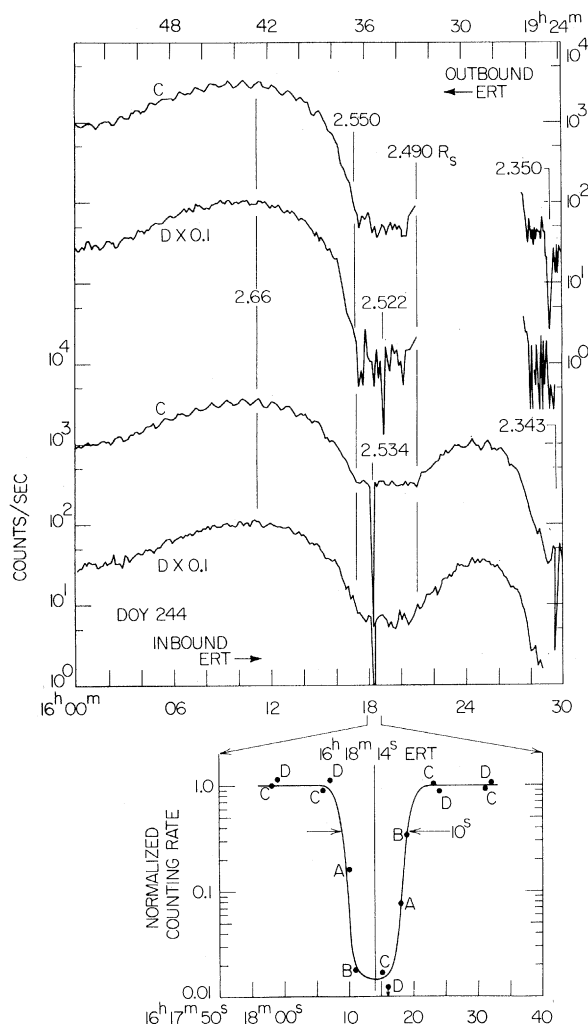


Fig. 4. Plots of frame-by-frame counting rates of C and D, inbound and outbound. The absorption feature at 16 hours 18 minutes 14 seconds ERT is shown on an enlarged scale in the lower panel for four detectors, whose ambient counting rates have been normalized to unity.

the geometric center of the planet, namely $0.02 R_S$ [see (8)].

Another principal feature of Fig. 5 is a marked absorption between 2.371 and $2.336 R_S$, centered at $2.35 R_S$, accurately confirmatory of a ring of disperse scattering material reported by the imaging team (13). They have called this feature the F ring and the region between it and the outer edge of the A ring the Pioneer division. We also confirm the existence of such a division. In addition, we find significant effects on the angular distribution of low-energy electrons (a relative absence of particles with mirror points near the equator) extending outward to at least $2.45 R_S$, suggesting a tenuous distribution of particulate matter.

Also, we find (Fig. 5) within the F ring a strong narrow absorption signature in detectors A, B, and C at $2.343 R_S$, characteristic of a satellite of diameter ≥ 100 km. We designate this as 1979 S 5.

Feibelman's E ring (also called the D' ring) is defined observationally (17) to lie in the equatorial plane between about 3.3 and $6.5 R_S$. We are unable to confirm its existence, but its influence on energetic particle distributions (18) may be obscured by the stronger effects noted above.

On the outbound leg of the trajectory, the telemetry signal was not reacquired after occultation by the planet until 1921:37 ERT ($2.301 R_S$). Hence, the rapid recovery from background rates within the central void of the magnetosphere was not observed, but the signature of the F ring was reconfirmed. A further satellite signature was observed outbound at $2.350 R_S$, at the 99 percent confidence level (1979 S 6). This signature may be the longitudinally extended shadow of 1979 S 5.

After the spacecraft entered the central void, data were acquired continuously in real time to 1756:30 ERT, that is, nearly to periapsis 1756:54.1 ERT ($1.349 R_S$). Thereafter for 51.2 minutes, data were stored at a total spacecraft bit rate of 16 bits per second and played back later over the telemetry link. The observed rates of all of our Geiger-Müller detectors within the void were slightly below the rates that we calculated for this epoch from the preflight data on the radioactive background of the radioisotope thermal generators (RTG's) that supply the electrical power for the spacecraft. The rate of the solid-state detector G was accurately equal to the rate of its americium-241 calibration source. Thus, the A, B, and C rings provide a very effective shield against magnetospheric particles. No particles were observed on the magnetic shell through Cassini's divi-

Fig. 5. Plots of frame-by-frame counting rates for A, B, and C, inbound.

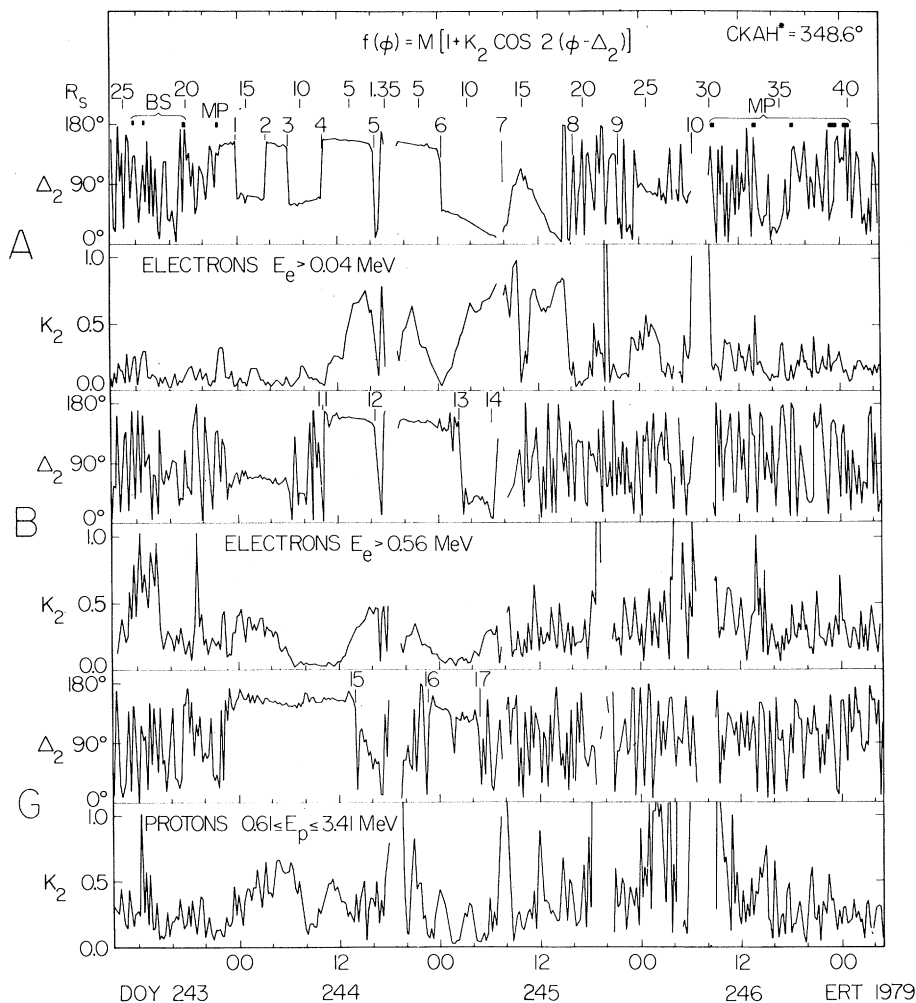
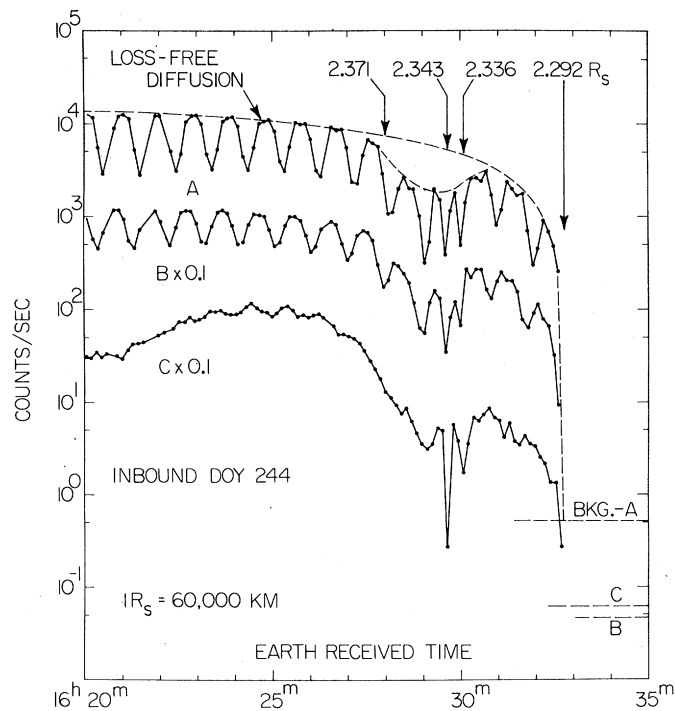


Fig. 6. Plots of 115.5-second values of the second-order anisotropy parameters K_2 and Δ_2 for A, B, and G for the entire encounter. The serial numbers 1, 2, 3, . . . 17 label transitions of interest.

$-d(\ln j)/d(\ln E)$ implied by corotation and the values measured directly by multi-channel detectors of the Goddard Space Flight Center group (19, 20).

Conclusions. In the interest of brevity, the various conclusions of the previous sections are not repeated here but an overview of them is given in the abstract.

J. A. VAN ALLEN, M. F. THOMSEN
B. A. RANDALL, R. L. RAIDEN
C. L. GROSSKREUTZ

Department of Physics and Astronomy,
University of Iowa,
Iowa City 52242

References and Notes

1. J. W. Dyer, *Science* **207**, 400 (1980).
2. L. W. Brown, *Astrophys. J.* **198**, L89 (1975).
3. M. L. Kaiser and R. G. Stone, *Science* **189**, 285 (1975).
4. J. A. Van Allen, D. N. Baker, B. A. Randall, D. D. Sentman, *J. Geophys. Res.* **79**, 3559 (1974).
5. J. A. Van Allen, B. A. Randall, D. N. Baker, C. K. Goertz, D. D. Sentman, M. F. Thomsen, H. R. Flindt, *Science* **188**, 459 (1975).
6. The detector complement of the University of Iowa Geiger tube telescope instrument comprises six miniature Geiger-Mueller tubes A, B, and C (EON Corporation type 6213) and D, E, and F (EON Corporation type 5107); and a single-element solid-state detector G (29 μm in thickness, totally depleted silicon). The single rates of A, B, C, D, and G and multiple coincidences AB, ABC, and DEF are transmitted. The directional detectors A, B, and G have conical physical collimators whose axes are perpendicular to the spin axis of the spacecraft. The spin axis is kept pointed at Earth to within about 1°. The spin period of the spacecraft was 7.693 seconds. During most of the encounter we obtained one 0.750-second sample of the counting rate of each of our ten detector channels at intervals of 8.25 seconds. A 360° angular distribution with nearly uniform spacing of samples was obtained each 115.5 seconds. Our instrument performed normally throughout the Saturn encounter and, because of the much lower counting rates than those in Jupiter's magnetosphere, only minor dead-time corrections were necessary for detectors A and B and none was necessary for the other detectors.

All positional data are taken from the post-encounter ephemeris [in ephemeris time (ET) at

- the spacecraft] prepared by the navigation section of the Jet Propulsion Laboratory (W. E. Kirhofer and W. H. Blume) and provided to investigators on 3 September. During the close-in portion of the trajectory the estimated accuracy of the radial distance from the spacecraft to the center of the planet is ± 60 km ($\pm 0.001 R_S$) and of planetocentric latitude is $\pm 0.02^\circ$ relative to the adopted polar axis of the planet $\lambda = 78.8142^\circ$, $\beta = 61.9324^\circ$ (ecliptic-equinox coordinates of 1950.0). The planetocentric longitude of the spacecraft is given for an adopted rotational period of 10 hours 14 minutes (sidereal) and an arbitrary prime meridian (that is, the hour angle of the vernal equinox of the planet measured from the adopted prime meridian of the planet was taken to be zero at 1950.0 ET). In this report, all times are Earth received times (ERT) [universal time (UT), referred to the Greenwich meridian] of the telemetry signal. At periapsis, $\text{ERT} = \text{ET} (\text{spacecraft}) - 50.2^{\text{sec}} + 86^{\text{min}} 20.5^{\text{sec}}$. The adopted unit of distance is the equatorial radius of the planet, $1 R_S = 60,000$ km.
7. J. H. Wolfe, J. D. Mihalov, H. R. Collard, D. D. McKibbin, L. A. Frank, D. S. Intriligator, *Science* **207**, 403 (1980).
 8. E. J. Smith, L. Davis, Jr., D. E. Jones, P. J. Coleman, Jr., D. S. Colburn, P. Dyal, C. P. Sonnett, *ibid.*, p. 407.
 9. M. H. Acuña and N. F. Ness, *ibid.*, p. 444.
 10. J. A. Simpson, T. S. Bastian, D. L. Chenette, G. A. Lentz, R. B. McKibbin, K. R. Pyle, A. J. Tuzzolino, *ibid.*, p. 411.
 11. W. Fillius, W. H. Ip, C. E. McIlwain, *ibid.*, p. 425.
 12. J. A. Van Allen and N. F. Ness, *J. Geophys. Res.* **74**, 71 (1969).
 13. T. Gehrels *et al.*, *Science* **207**, 437 (1980).
 14. J. W. Fountain and S. M. Larson, *Icarus* **36**, 92 (1978).
 15. K. Aksnes and F. A. Franklin, *ibid.*, p. 107.
 16. A. P. Ingersoll, G. S. Orton, G. Neugebauer, G. Münch, S. C. Chase, *Science* **207**, 439 (1980).
 17. W. A. Feibelman, *Nature (London)* **214**, 793 (1967).
 18. M. F. Thomsen and J. A. Van Allen, *Geophys. Res. Lett.* **6**, 893 (1979).
 19. A. L. Schardt, private communication.
 20. J. H. Trainor, F. B. McDonald, A. W. Schardt, *Science* **207**, 421 (1980).
 21. This work was supported in large part by Ames Research Center/NASA contract NAS2-6553 and the U.S. Office of Naval Research. We are indebted for assistance in many ways to C. F. Hall, R. P. Hogan, and R. O. Fimmel of the Ames Research Center; to R. L. Brechwald, D. D. Sentman (now at UCLA), R. F. Randall, D. E. Cramer, H. D. Owens, E. A. Freund, and E. D. Robison of the University of Iowa.

3 December 1979

Observations of Energetic Ions and Electrons in Saturn's Magnetosphere

Abstract. *The passage of Pioneer 11 by Saturn provided a detailed view of a planetary magnetosphere that is intermediate between those of Jupiter and Earth in both scale and the complexity of its dynamic processes. It appears to have at least three distinct regions: (i) an outer magnetosphere, extending from 17 to 7.5 Saturn radii, that resembles that of Earth in many important aspects; (ii) a slot region, between 7.5 and 4 Saturn radii, where a marked decrease in all protons and low-energy electrons is observed; and (iii) an inner region, extending from 4 Saturn radii to the ring edge, that features a sharp increase in the proton flux extending to energies greater than 20 million electron volts. A cutoff of both proton and electron fluxes occurred just beyond the nominal edge of the A ring.*

Data from the cosmic-ray experiment conducted by the Goddard Space Flight Center and the University of New Hampshire during the recent Pioneer 11 flyby of Saturn reveal a complex but moderately sized magnetosphere in which the planetary moons, rings, and temporal effects play key roles. This re-

port summarizes our first direct observations of the magnetosphere of this giant planet. The experiment provides detailed proton energy spectra and angular distributions from 0.2 to 22 MeV and electron energy spectra and angular distributions from 0.1 to 2 MeV. In addition, helium nuclei are measured in several intervals

between 0.65 and 22 MeV per nucleon (1). The spacecraft approached the Saturn system near the subsolar point and exited toward the dawn meridian (2). An overview of the energetic particle data is provided by the proton and electron time histories for three different energies of each component (Figs. 1 and 2). This limited spatial survey suggests a tentative division into three distinct regions:

1) Outer magnetosphere [magnetopause to 7.5 Saturn radii (R_S)]: this region is characterized by monotonically increasing fluxes and hardening of the spectra inward from the magnetopause. There are large and unusual changes in the angular distributions of low-energy electrons.

2) Slot region (7.5 to 4 R_S): the proton flux decreases by a factor of 50 and the low-energy electron flux by a factor of at least 10. The Saturn moons Dione, Tethys, and Enceladus, which orbit this region, appear to play major roles in reducing the fluxes.

3) Inner magnetosphere (4 R_S to nominal A ring edge): the proton fluxes increase rapidly inside the orbit of Enceladus, with deep flux depressions observed near the orbits of Mimas, Janus, and possibly S 11. The rapid proton increase extends to energies greater than 20 MeV and the proton energy spectra become complex. A sharp cutoff of all trapped particles was observed at the ring edge.

Prior to the encounter, no measurable fluxes of energetic ions or electrons were detected that could be attributed to Saturn. Thus there is no indication that Saturn's magnetosphere is a source of interplanetary electrons, as is Jupiter's (3, 4). A moderately sized solar cosmic-ray event was in progress during the encounter period, and fluxes of 10- to 20-MeV protons were detected in the outer magnetosphere. It is plausible that these were of solar cosmic-ray origin and had access to the magnetosphere via a Saturn tail region in the same manner that low-energy solar cosmic rays penetrate deep into Earth's magnetosphere (5). Studies are being carried out to determine how well the Saturn tail region can be defined by these observations.

In the following discussion, the three regions of the Saturn magnetosphere are described in greater detail.

Outer region. The time histories for 0.2-, 0.7-, and 1.2-MeV protons and 0.1-, 0.8-, and 1.1-MeV electrons in the outer region are shown in Figs. 1 and 2. The magnetopause was first encountered in the subsolar region at 17.3 R_S and is an effective boundary for particles of low rigidity (0.2-MeV protons and 0.5-MeV